Anal. Chem. **2001,** *73,* 732−739

Articles

Multispectral Imaging Microscope with Millisecond Time Resolution

Oleg Khait, Sergey Smirnov, and Chieu D. Tran*

Department of Chemistry, Marquette University, P.O. Box 1881, Milwaukee, Wisconsin 53201

A new multispectral imaging microscope with micrometer spatial resolution and millisecond temporal resolution has been developed. The imaging microscope is based on the use of an acousto-optic tunable filter (AOTF) for spectral tuning and a progressive scan camera capable of snapshot operation for recording. It can operate in two modes: images are recorded as a function of time or wavelength. When operated as a function of time, the microscope is configured so that as many images as possible are recorded, grabbed, and stored per one wavelength. Upon completion, the AOTF is scanned to a new wavelength, and a new set of images are recorded. Up to 33 images/second (i.e., 30 ms/image) can be recorded in this mode. In the other configuration, the recording wavelength is rapidly scanned (by means of the AOTF) and only one image is rapidly recorded, grabbed, and stored for each wavelength. Because additional time is needed to scan the AOTF, the maximum number of images can be grabbed in this case is 16 frames/s. Preliminary applications of the imaging microscope include measurements of photoinduced changes of a single unit cell in temperature-sensitive cholesteric liquid crystals as a function of time and wavelength. The changes were found to be varied with time and wavelength. Interestingly, the photoinduced changes of unit cells in the liquid crystal are not the same but different from cell to cell. This imaging microscope is particularly useful for measurements of small-size samples that undergo rapid chemical or biochemical reactions, e.g., activities of a single biological cell.

Multispectral imaging is a technique that can simultaneously record spectral and spatial information of a sample; i.e., the recorded images contain signals that are generated by a sample, plotted as a function of spectral and spatial distribution.[1] Instruments that can perform these tasks have been developed recently. They are based on the use of either an electronic tunable filter (acousto-optic tunable filters[2−4] or liquid crystal tunable filters[5]) or an FT-IR[6−8] for spectral scanning and an area camera (silicon,[2] InGaAs,[3] InSb,[4] HgCdTe[6,7]) for image recording. Studies that to date were not possible can now be performed using these newly developed instruments. These include the determination of the chemical inhomogeneity of polymers,[3,9] the authentication of stock certificate and currency,[3] the evidence of kinetic inhomogeneity,[10] and the detection of solid-phase peptide synthesis mediated by solid-phase combinatorial chemical method.[11] The technique is not limited to the macroscopic-scale samples. By incorporating a microscope into the mutispectral imaging instrument, microscopic imaging has been achieved.[4,5]

It is desirable to increase the speed of the multispectral imaging microscope. Faster speed will make it possible to study fast chemical, biochemical, or photochemical reactions of a single unit cell in a sample. Such a study is important because it has been reported that activities of cells may not be homogeneous but rather are different from cell to cell. Unfortunately, it is not possible to perform this type of study using reported multispectral imaging instruments[4,5] because these instruments have rather slow temporal resolution (seconds or minutes). A faster imaging instrument cannot be constructed by simply arranging commercially available components. In fact, many factors need to be addressed in order to increase the speed of the instrument. They include the speed of the spectral scanning device, the camera, and the frame grabber. The liquid crystal tunable filter (LCTF)[5]and acousto-optic tunable filter (AOTF)[12,13] are two of the fastest electronic tunable filters currently available. Between them, AOTF is relatively faster than the LCTF because the tuning speed of the former is based on the speed of sound in a crystal, which is on the order of microseconds, whereas the latter is on the response of the liquid crystal, which is on the order of milliseconds.[12,13] In addition to fast recording speed, it is essential that a camera can be externally controlled (i.e., trigger) so that recorded images can be synchronized with events occurring in

(1) Morris, M. D. *Microscopic and Spectroscopic Imaging of the Chemical State*; Marcel Dekker: New York: 1993.
(2) Treado, P. J.; Levin, I. W.; Lewis, E. N. *Appl. Spectrosc.* **1992**, *46*, 553−559.
(3) Tran, C. D.; Cui Y.; Smirnov, S. *Anal. Chem.* **1998**, *70*, 4701−4708.
(4) Treado, P. J.; Levin I. W.; Lewis, E. N. *Appl. Spectrosc.* **1994**, *48*, 607−615.
(5) Morris, H. R.; Hoyt, C. C.;. Treado, P. J. *Appl. Spectrosc.* **1994**, *48*, 857−866.
(6) Lewis, E. N.; Treado, P. J.; Reeder, R. C.; Story, G. M.; Dowrey, D. E.; Marcott, C.; Levin, I. W. *Anal. Chem.* **1995**, *67*, 3377−3381.
(7) Lewis, E. N.; Gorbach, A. M.; Marcott, C.; Levin, I. W. *Appl. Spectrosc.* **1996**, *50*, 263−269.
(8) Lewis, E. N.; Kidder, L. H.; Arens, J. F.; Peck, M. C.; Levin, I. W. *Appl. Spectrosc.* **1997**, *51*, 563−567.
(9) Snively, C. M.; Koening, J. L. *Macromolecules* **1998**, *31*, 3753−3755.
(10) Fischer, M.; Tran, C. D. *Anal. Chem.* **1999**, *71*, 953−959.
(11) Fischer, M.; Tran, C. D. *Anal. Chem.* **1999**, *71*, 2255−2261.
(12) Tran, C. D. *Anal. Chem.* **1992**, *64*, 971A−981A.
(13) Tran, C. D. *Talanta* **1997**, *45*, 237−248.

10.1021/ac0007581 CCC: $20.00
Published on Web 01/03/2001

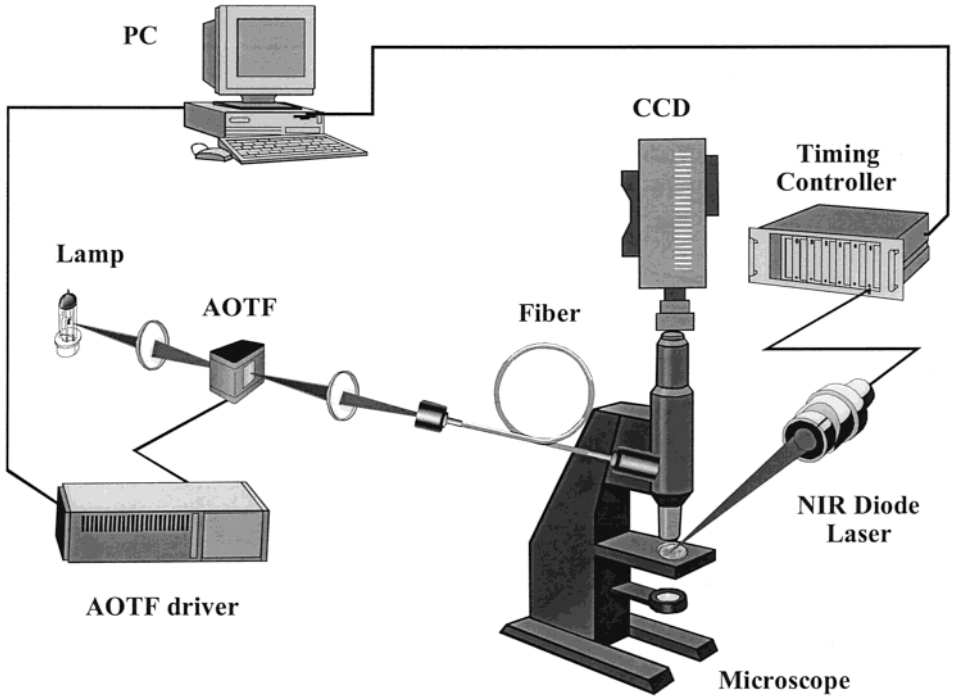

Figure 1. Schematic diagram of the microscopic multispectral imaging instrument.

the sample. Such requirements can be satisfied with cameras that have become commercially available recently. These high-performance cameras have high sensitivity and can rapidly record images. They also can operate in the "snapshot" mode, whichenables the use of an external signal to trigger the recording of a single image or images.

It is often wrongly assumed that faster recording of images can be simply accomplished by use of a fast camera. While it is true that a fast camera is essential for such an instrument, a faster camera does not necessarily mean that images can be rapidly recorded. This is due to the fact that the images captured by the camera must be rapidly grabbed and then rapidly transferred out of the camera so that the camera can retain its speed without any dead time. As a consequence, the role of the frame grabber is essentially important in the fast spectral imaging instrument. Since all commercially available frame grabbers come with rather simple and basic software that does not have these features, elaborated and complex procedures, including controlling and synchronizing the timing as well as developing of complicated and extensive programs for the frame grabber, must be developed in order to increase the temporal resolution of the spectral imaging instrument.

The information presented is indeed provocative and clearly indicates that it is possible to use the AOTF, a "snapshot" camera together with a frame grabber equipped with novel and elaborated electronics and programs to construct a new multispectral imaging microscope that can rapidly record images of a single unit cell in a sample. The instrumentation development of the multispectral imaging microscope and its utilization to study changes of submicrometer unit cells in liquid crystals induced by irradiation with a near-infrared pulsed laser are reported in this paper.

EXPERIMENTAL SECTION

Time-resolved multispectral microimaging of sample was performed with the instrument shown in Figure 1. As illustrated, a microscope (Carl Zeiss model) was incorporated into the imaging instrument to facilitate microimaging, i.e., to record time-resolved multispectral images of a single-crystal unit of 3−5 μm in the liquid crystal film. The sample placed on the microscope table was irradiated with a a single-mode 805-nm diode laser. This laser, which was powered by an ILX Lightwave power supply (model LDX 3565), can be operated in either continuous or pulse mode with adjustable pulse lengths. A combination of two lenses with focal lengths of 8 and 60 mm was used to focus the near-infrared (NIR) laser beam. When it was operated in the cw mode, the beam spot size was adjusted to be ∼1 mm. A much smaller beam (∼25 μm) was used when the laser was in the pulse mode. A smaller beam spot size was needed in this case in order to concentrate the laser power to provide adequate signal for measurements. When excited by the cw NIR laser with 1-mm beam spot size, many unit cells in the liquid crystal sample were simultaneously excited. This is because each unit cell in the liquid crystal is about 3−5 μm diameter in size. Changes in the sample induced by the NIR diode laser irradiation were measured by use of a 250-W halogen tungsten lamp as the light source. White light from the W lamp was spectrally tuned by a TeO_2 noncollinear acousto-optic tunable filter (Matsushita Electronics model EFL-F20R2). A home-built rf driver [14] was used to drive the AOTF. Light diffracted from the AOTF was directed to the sample by mean of a 5-mm-diameter liquid light guide (Lumatec Gmbh, Munich, model S-2000). A microscope objective lens with 20× magnification was used to focus the illumination light into the sample and also to collect light reflected from the sample. An 8-bit 512 × 512 (10 μm × 10 μm pixel size) progressive scan silicon area camera (Dalsa Corp. model CA-D8) was used to recorded images. This camera operated in the snapshot mode; namely, the images recording was triggered by an external signal generated by the computer. In this imaging microscope, the two objective

(14) Tran, C. D.; Lu, J. *Appl. Spectrosc.* **1996**, *50*, 1578−1584.

lenses offer a combined magnification of 25× (1.25× and 20×). The spatial resolution of the imaging microscope is also derived from the camera, which has 512 × 512 pixels with 10 μm × 10 μm size. It is estimated that the instrument should, in principle, have a spatial resolution of ~0.5 μm. However, because of the diffraction limited, the microscope resolution should be ~1.5 μm (resolution $1.22\lambda/\mathrm{NA}$, where $\lambda = 600$ nm and NA = 0.5). Because each unit cell of the liquid crystal has a dimension of 3−5 μm, they can be individually measured by the imaging microscope. A digital frame grabber (Dipix Corp. model XPG-1000) was used to grab images from the camera for subsequent transfer to the computer for imaging processing. Software written in C++ language was used to control and to synchronize the timing of the instrument, to control the frequency and the power, and to scan the applied rf signal. The same software also facilitates grabbing images from the camera, storing them in the memory (of the frame grabber) for subsequent transferring to the computer for analysis.

A set of temperature-sensitive liquid crystal sheets was purchased from Edmund Scientific. According to the manufacturer, the sheets were produced by dispersing 3−5 μm size crystals cholesteric liquid crystal in a polymer matrix. In each sheet, the film was encapsulated between two sheets of Mylar for protection. One side of the sheet was coated with black ink.

RESULTS AND DISCUSSION

Three different cholesteric liquid crystal sheets used in this study were specified by the manufacturer to be sensitive to four different temperature ranges: 30−35, 35−40, and 40−45 °C. Each sheet is known to contain dispersion of unit cells of 3−5 μm size. They are, therefore, particularly suited for this study because each unit cell can be individually observed by the microcopic multispectral imaging instrument.

The liquid crystals absorb near-infrared light because they are composed of organic compounds and these compounds absorb NIR light through the overtone and combination absorption of the C−H, O−H, and N−H groups.[15,16] As a consequence, irradiating the liquid crystal with a NIR laser at 805 nm leads to a change in its temperature, which, in turn, produces changes in the absorption and refractive index. Since changes generated are in the visible region, they can be readily monitored with a visible silicon CCD. As this is an area camera, each recorded image corresponds to a three-dimensional picture of the sample. It can, therefore, be used to record rapid changes in the liquid crystal either as a function of wavelength (i.e., rapidly record images at different wavelength at a constant time) or as a function of time (i.e., quickly record picture at a fixed wavelength as a function of time) but not both (i.e., simultaneously varying both time and wavelength). This is because changes in the absorption and refractive index of the liquid crystal with time are faster than the time required to change the wavelength setting of the AOTF and to record a new image. As a consequence, two sets of experiments were designed to demonstrate the operation of the image spectrometer and the properties of the liquid crystal: images were recorded as a function of wavelength and as a function of time.

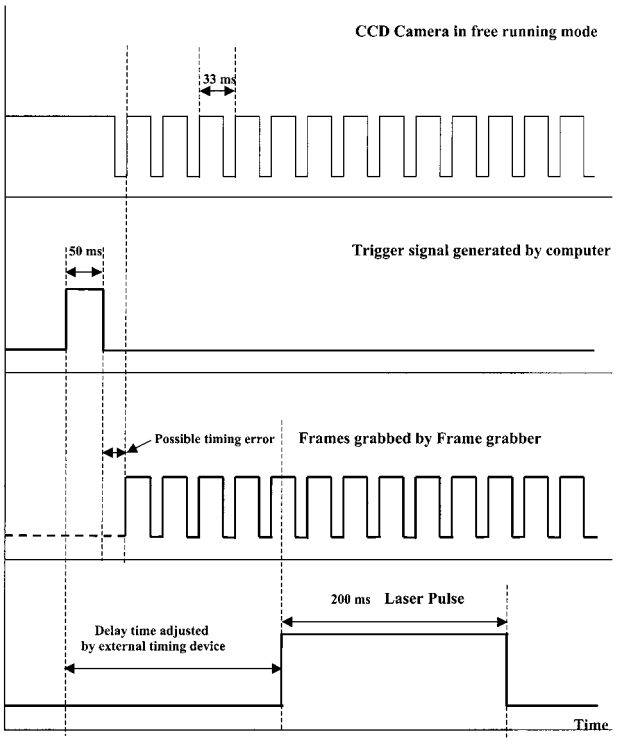

Figure 2. Timing sequence of the multispectral imaging microscope for recording images as a function of time.

In the first set of experiments, the liquid crystal was irradiated with light at 805 nm from a NIR diode laser operated in the pulse mode. Changes in the sample were monitored by rapidly and consecutively recording multiple images as a function of time at a single wavelength. Subsequently, the recording wavelength was changed and a new set of images were recorded. The procedure was repeated for several wavelengths so that subsequent treatment of images will enable the calculation of spectra that show the changes as a function of time (for each illuminating wavelength).

In the second set of experiments, the liquid crystal was irradiated with the same NIR diode laser but the laser was operated in the continuous mode. Because it was continuously irradiated with the cw light, the photoinduced changes in the liquid crystal reached a steady-state condition; namely, there should be no changes as a function of time. As a consequence, it was possible to investigate changes as a function of wavelength. This was accomplished by concurrently illuminating the sample with a monochromatic light from the AOTF. An image of the light reflected from the sample was recorded at this wavelength. The AOTF was then scanned rapidly to the next wavelength where another image was recorded. The process continued until a whole set of *n* images were recorded for n different wavelengths.

1. Multispectral Imaging as a Function of Time. The first set of experiments were designed to study the rapid photoinduced changes in the liquid crystals as a function of time (at a fixed wavelength). This was accomplished by irradiating the sample with the 805-nm diode laser operated in the pulse mode. Changes produced were monitored by the illuminating monochromatic light from the AOTF. Timing of the experiments is shown in Figure 2. The computer generated a pulse (trace 2 of Figure 2), and the positive slope of the pulse triggered the diode laser. The laser diode can be set to fire either immediately (by the positive slope

(15) Tran, C. D.; Grishko, V. I.; Baptista, M. S. *Appl. Spectrosc.* **1994**, *48*, 833−842.
(16) Baptista, M. S.; Tran, C. D.; Gao, G. H. *Anal. Chem.* **1996**, *68*, 971−976.

of this pulse) or at any appropriate time by inserting a delay time which is provided by the timing control unit (trace 4). The Dalsa CCD camera was operated in the free running mode; namely, it continuously recorded images (trace 1). The negative slope of the pulse generated by the computer started the frame grabber (trace 3). The frame grabber was operated in the multiple grabbing mode; namely, it was set to acquire a set of multiple and consecutive images as fast as it could grab them from the camera (for a set duration, which in this study was 1.5 s). These frames were then consecutively stored in the memory of the frame grabber board. Again, similar to the first set of experiments, the maximum number of frames that the frame grabber can grab in a given time is dependent on a variety of factors including the total number of frames stores in the frame grabber (i.e., the memory of the frame grabber board and the size of each frame), the speed to transfer the frames, and the specifications of the camera (the exposure time). This number is higher than that for the first set of experiments because images were recorded at a fixed wavelength; i.e., the switching time of the AOTF was not required in this case. The maximum number of frames that the grabber can grab was determined to be 33 frames/s. Therefore, a total of 50 images can be grabbed by the grabber in the 1.5-s duration set in this study.

As described above, by use of the signal generated by the computer and the delay line provided by the timing controller, the firing of the diode laser pulse can be precisely controlled. However, because the CCD camera was operated in the free running mode and the frame grabber was triggered by the negative slope of the same computer-generated signal, it was difficult to precisely control the start of the frame grabbing. This is because the grabber can only grab a whole frame from its beginning. As a consequence, there may by some errors due to this timing mismatch (trace 3). However, error produced by this mismatch is not more than one frame, i.e., ±15 ms.

As illustrated in Figure 2, four images of the sample were recorded and grabbed prior to the laser pulse. However, the number of images that are recorded before the laser pulse is not fixed at four frames as illustrated. It can be appropriately adjusted by the delay line. As a consequence, events occurring in the sample can be monitored at any time (i.e., before, during, and after the laser pulse) and for any duration of time. This timing arrangement makes it possible to precisely determine the timing of the experiment, namely, the time $t = 0$ when the laser pulse is incident onto the sample. It also offers background images (i.e., image of the sample before the photoinduced changes) which can be used for background correction. In this study, the laser pulse width was 200 ms. Therefore, there were about five or six images of the sample during the time the laser pulse was irradiating it. Image 11 and thereafter are those of the sample after the laser pulse went off. From the same area, which in this case corresponds to a square of 7 × 7 pixels, the intensity of the reflected light was calculated from each of the images beginning with image 11. This allows the construction of the spectra that show the changes of the sample as a function of time.

Shown in Figure 3A are the results obtained for a single unit cell of the 30−35 °C liquid crystal. As illustrated, changes in the intensity of light reflected from the cell at different illumination wavelengths were plotted as a function of time. About 500 ms after

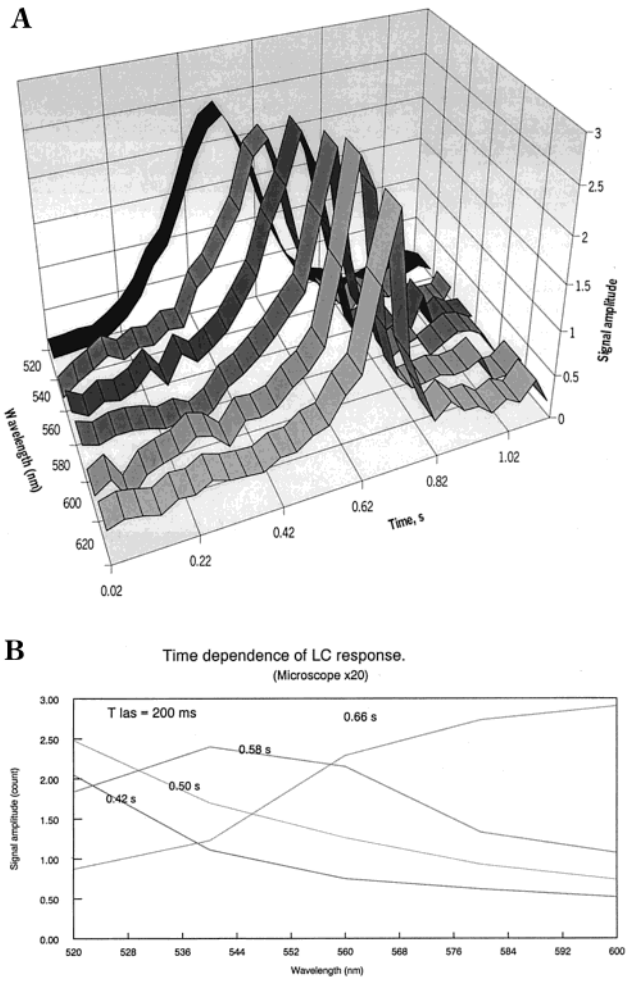

Figure 3. (A) Changes in the reflected light intensity at different wavelengths, plotted as a function of time, for a single cell in the 30−35 °C liquid crystal sample and (B) changes in the reflected light intensity measured at different times after the laser pulse, plotted as a function of wavelength for a single cell in the 30−35 °C liquid crystal sample.

the NIR laser pulse, the cell underwent changes in the visible-region around 520 nm. The changes shifted toward longer wavelength concomitantly with time, i.e., maximum changes at about 730 ms shifted to 620 nm. Interestingly, initial changes in the shorter wavelength region at the beginning decay relatively slower than those at the longer wavelengths at the later time; i.e., the slopes were relatively smaller for bands at shorter wavelengths than those for bands at longer wavelengths.

The effect can be seen clearer in Figure 3B, which was constructed from the data in Figure 3 showing, as a function of wavelength, the response of the liquid crystal at three different times (420, 500, and 660 ms) after the laser pulse. As illustrated, 420 and 500 ms after the laser pulse, the changes in the liquid crystal decreased rapidly as a function of wavelength. However, 660 ms after the laser pulse, the intensity of the reflected light increased as a function of wavelength. However, the slope of the buildup at the longer time scale is smaller than that of the decay of the shorter time.

It is important to point out that change in the temperature is known to produce changes in the absorption and the refractive

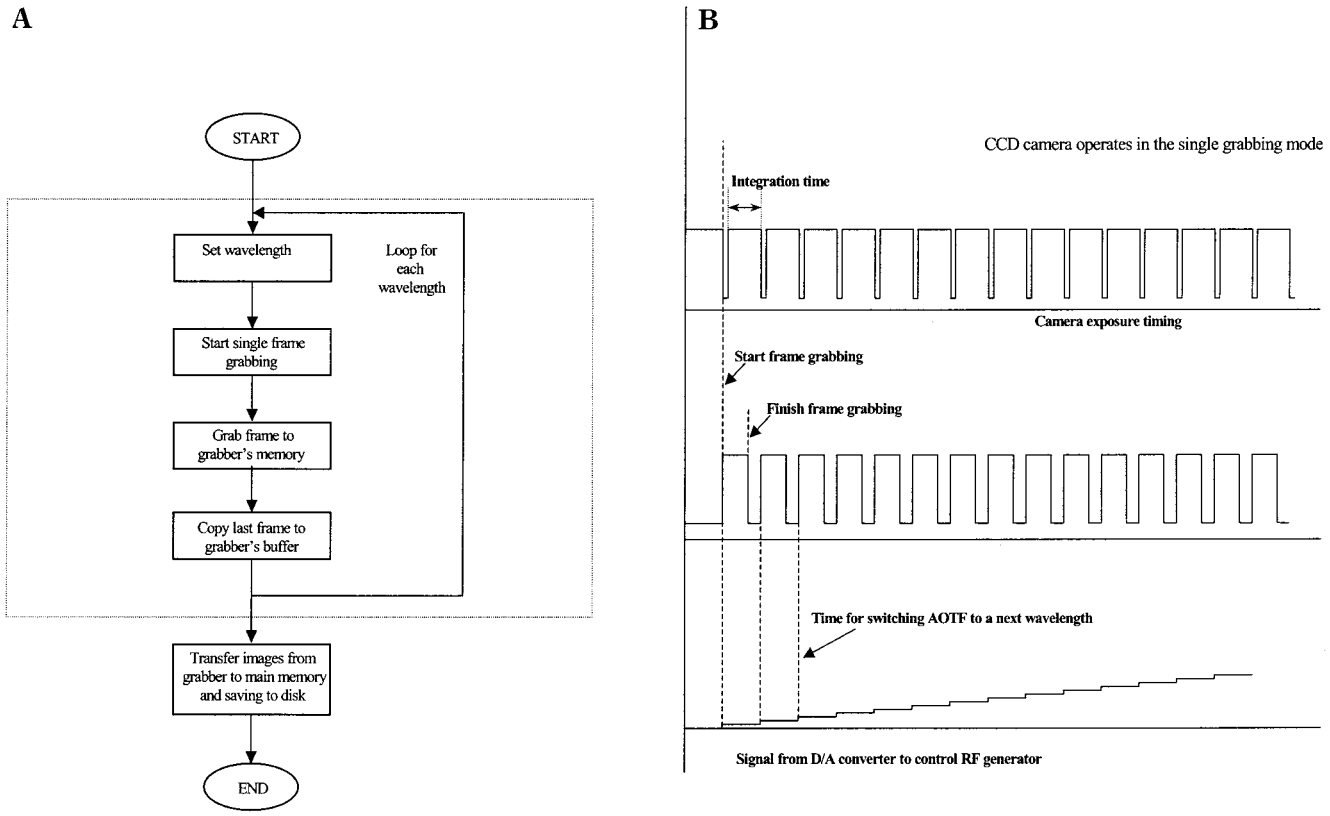

Figure 4. Flowchart (A) and timing sequence (B) of the multispectral imaging microscope for recording images as a function of wavelength.

index of liquid crystals.[17,18] Because, in this experiment, the intensity of the light diffuse-reflected from the sample was measured, it is not possible to separate the change in the absorption from that of the refractive index.

2. Multispectral Imaging as a Function of Wavelength. The experiments were designed to demonstrate that the imaging spectrometer is capable of rapidly recording images at different wavelengths. As described in the previous section, this was accomplished by simultaneously irradiating the liquid crystal with the cw NIR diode laser and the monochromatic light from the AOTF and rapidly scanning the AOTF to change the wavelength of the illuminating light. The flowchart and timing sequence are shown in Figure 4A and B. The Dalsa CCD camera was operated, not in the free running mode as in the previous experiments but rather in the snapshot mode; namely, it was triggered by an external signal generated by the computer. This computer-generated pulse also started the frame grabber. The frame grabber rapidly grabbed one recorded image and then rapidly copied it into the next available buffer in its memory for storing. The time spent during this frame transfer enabled the AOTF to be switched to the next wavelength. Again an image at this wavelength was grabbed and transferred to the grabber's memory for storage. The process continued (i.e., one frame per one wavelength) until the frame grabber memory was full of frames. At that time, all of the stored frames were transferred to the computer.

The maximum number of frames that can be stored is dependent on a variety of factors including the scanning speed of the AOTF, the memory of the frame grabber board, and the size of each frame as well as the exposure time (i.e., the integration time) of the camera. The maximum number of frames that the grabber can grab was found to be 16 frames/s (62.5 ms for one image at one wavelength).

3-D and 2-D plots of an image of the 30−35 °C liquid crystal taken at 550 nm are shown in Figure 5A and B, respectively. To take this picture, a lens was used to focus the NIR laser diode beam to a spot size of ~250 μm. Since the size of the unit cell in the liquid crystal is about 3−5 μm, many cells were simultaneously irradiated by the laser beam. The cells and the dispersing medium have different absorption and thermal physical properties because they are composed of different chemical. These differences produce contrast which enables the recording of the cells as dark spots in the 2-D plot (Figure 5B) and bands in the 3-D plot (Figure 5A). It was possible to simultaneously record many cells in this picture because the microscope was zoom-out to enable the CCD camera to record the whole sample. As illustrated, the liquid crystal liquid crystal contain cells with various sizes ranging from about 3 to 7 μm. The magnitude of the photoinduced changes is proportional to the temperature changes produced as a consequence of the sample absorption of the NIR laser light. The absorption, in turn, is proportional to the size of the cell. Bands with different magnitudes were, therefore, observed as a consequence of size distribution of the cells.

Subsequently, the microscope was zoom-in to facilitate the recording of images of three largest individual cells. These are the three marked cells in the Figure 5. The AOTF was also rapidly scanned from 500 to 620 nm at 2-nm intervals. A total of 60 images were needed to construct one spectrum, which shows the change

(17) Jacobs, S. D. *Liquid Crystals for Optics*; SPIE Publishing: Bellingham, WA, 1992

(18) Drzaic, P. S. *Liquid Crystal Dispersions*; World Scientific Publishing: River Edge, NJ, 1995.

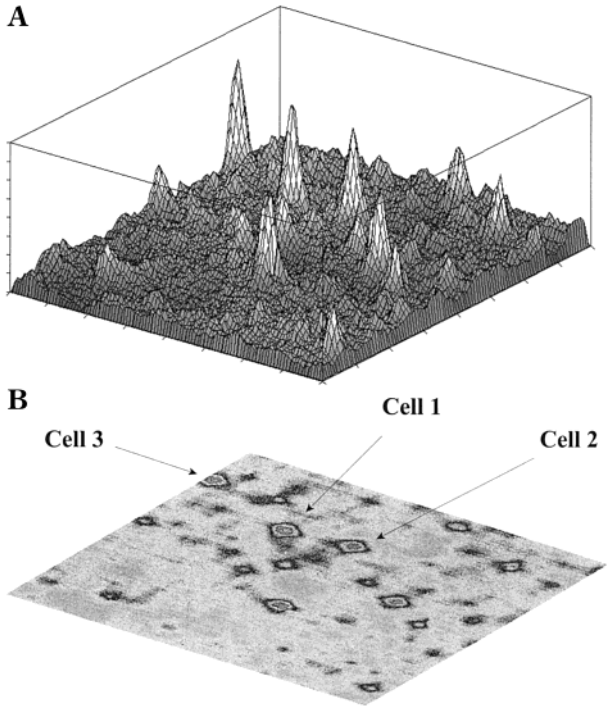

Figure 5. 3-D (A) and 2-D (B) plots of images of reflected light intensity at 600 nm taken when many unit cells of the 30−35 °C liquid crystal sample were simultaneously irradiated by the 805-nm cw diode laser.

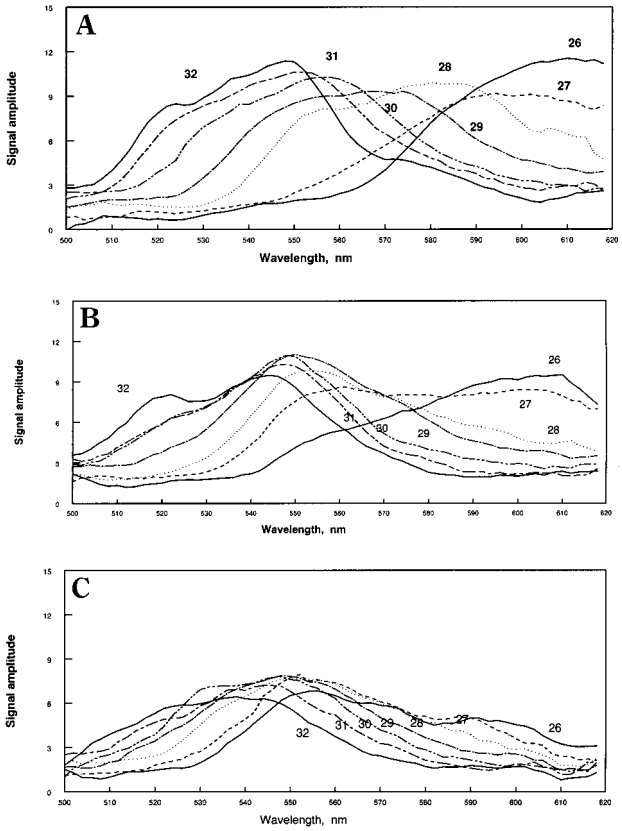

Figure 6. Changes in the reflected light intensity as a function of wavelength for three different individual unit cells in the 30−35 °C liquid crystal, at different irradiating diode laser powers (from 26 to 32 mW). These are the three cells marked in Figure 5.

in the intensity of the reflected light as a function of wavelength. As described in the previous paragraph, in this configuration, the instrument can grab 16 frames/s. As a consequence, it required 3.75 s to acquire 60 images from which one spectrum was calculated. Three different cells in the 30−35 °C sample were separately measured, and different irradiating laser powers (from 26 to 32 mW) were used for each cell. Spectra of each cell at different laser powers were calculated from recorded images. The calculated spectra were then corrected for the differences in the intensity of the illuminating halogen tungsten lamp, and the resulting spectra are shown in Figure 6A−C. The correction was necessary because it is known that the spectral output of the halogen tungsten lamp is dependent on wavelength. The correction was accomplished by replacing the sample with a mirror to record the spectral output of the tungsten lamp for the subsequent correction (by dividing the sample spectrum by the corresponding lamp spectral output). As illustrated in Figure 6A, increasing the power of the NIR irradiating laser light shifted the spectra toward shorter wavelength: the peak at ∼610 nm which was obtained with a 26-mW laser power shifted toward a shorter wavelength region to a very broad, unresolved band that centered at ∼570 nm when the laser power was increased to 28 mW. This unresolved broad band further shifted to about 560, 555, and 550 nm when the laser power was increased to 30, 31, and 32 mW, respectively (Figure 6A). This observation can be explained by the fact that increasing the power of the irradiating laser provides higher temperature change in the sample, which as a consequence shifts the changes toward shorter wavelength (higher energy) region.

It is of particular interest to observe in Figure 6 that, for the same 30−35 °C sample, different cells response differently. Largest changes with the laser power were observed for the cell shown in Figure 6A whereas the changes in the cell shown in Figure 6C are the smallest. This may be due to the differences in the sizes of the cells. As shown in Figure 5, there are a slight differences in the sizes of the cells from which the signals were recorded. Because of the diffraction and scattering of light from the cells, it is difficult to determine the exact differences in their sizes. The changes measured were produced by the temperature gradient which was generated by the cells' absorption of the NIR laser light. In addition to the laser power, the temperature gradient is also dependent on the thermal conductivity of the medium. Since the thermal conductivity of the cells is different from the dispersing medium, and changes for each cell were measured when the heat generated was equilibrated over the entire cell, it is expected that cells with different sizes will produce different signals.

Changes observed for the single cells in the 35−40 and 40−45 °C sample are similar to those for the 30−35 °C sample (Figure 7). For the 35−40 °C sample (Figure 7A), a single band at 580 nm was observed when the sample was irradiated with 29-mW laser power. The band became broad, unresolved, and shifted toward the shorter wavelength region when the laser power was increased to 31 mW. Thereafter, it continued to shift toward shorter wavelength. At 36-mW laser power, the band is broad and unresolved with one peak at ∼525 nm and the other is at a wavelength shorter than 500 nm. The response of the 40−45 °C sample (Figure 7B) is similar to that of the 25−30 °C and the 30−35 °C sample.

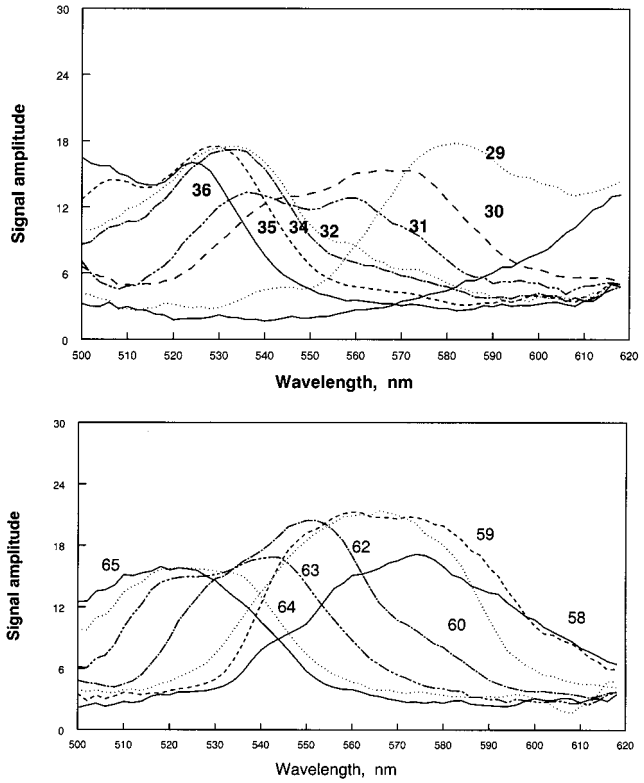

Figure 7. Changes in the reflected light intensity as a function of wavelength, at different irradiating laser powers for a single unit cell in the 35−40 °C liquid crystal (A) and the 40−45 °C liquid crystal (B).

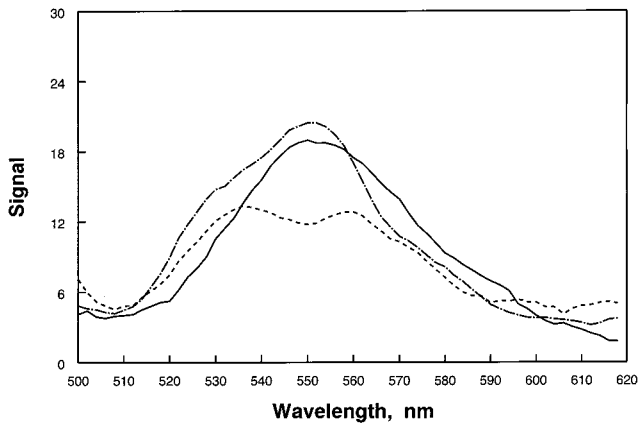

Figure 8. Changes in the intensity of the light reflected from a single unit cell in the 30−35 °C liquid crystal (—), the 35−40 °C unit cell (- - -), and the 40−45 °C unit cell (— . —), irradiated with a cw diode laser with 20, 32, and 52 mW power, respectively.

It is of particular interest to plot the response of single cells in the three samples in one graph (Figure 8). The spectra plotted in this figure were obtained with different laser powers: 19, 32, and 62 mW for the 30−35C, 35−40, and 40−45 °C samples, respectively. As illustrated, only 19-mW laser power was needed to produce change with a maximum at ∼550 nm for the 30−35 °C sample. Much higher power (32 and 62 mW) was required to produce change at the same wavelength region for the 35−40 and 40−45 °C sample, respectively. These results are as expected because higher laser power is needed to generate temperature change that is high enough to produce change in the higher temperature liquid crystals (35−40 and 40−45 °C).

In summary, we were able to develop a new multispectral imaging microscope with micrometer spatial resolution and millisecond time resolution by judicious use of an AOTF for spectral tuning and a progressive scan camera capable of snapshot operation for rapidly recording of images. The imaging microscope has a rather fast temporal resolution because in addition to the aforementioned hardware, we also developed novel, sophisticated, and elaborate electronic controlling device and software to control and synchronize the timing and to rapidly transfer images from the camera to the frame grabber's memory (for subsequent storing in the computer). Images that were captured by the camera were rapidly removed (from the camera) and transferred to the grabber's. This, in effect, avoids dead time in the camera and makes it possible for the imaging microscope to have millisecond time resolution.

The imaging microscope can be operated in two modes: images are recorded as a function of time or wavelength. When operated as a function of time, the microscope is configured so that as many images as possible are recorded, grabbed, and stored per one wavelength. Upon completion, the AOTF is scanned to a new wavelength, and a new set of images are recorded. Up to 33 images/s (i.e., 30 ms/image) can be recorded in this mode. Because the recording camera is synchronized with an external signal and a delay time can be installed to appropriately adjust the duration between the start of an event and the recording and grabbing of the image, the time resolution of the spectrometer is not limited to 20 ms but rather can be adjusted to a shorter or longer time scale. In the other configuration, the recording wavelength is rapidly scanned (by means of the AOTF) and only one image is rapidly recorded, grabbed, and stored for each wavelength. Because additional time is needed to scan the AOTF, the maximum number of images can be grabbed in this case is 10 frames/s.

Preliminary applications of the imaging microscope include measurements of photoinduced changes of a single unit cell in temperature-sensitive cholesteric liquid crystals as a function of time and wavelength. It was found that irradiating with a pulsed NIR diode laser of 805 nm led to changes in each unit cell of the liquid crystal. The changes were found to be varied with time and wavelength, namely, ∼500 ms after the NIR laser pulse, the liquid crystal underwent changes in the visible region around 520 nm. The spectrum shifted toward longer wavelength concomitantly with time, i.e., maximum at ∼730 ms shifted to 620 nm. Under steady-state conditions, i.e., when they were irradiated with a cw NIR diode laser, the liquid crystals underwent changes that were varied with the laser power. Specifically, for the 30−35 °C liquid crystal, the maximum change at 550 nm was obtained with only 20-mW irradiating power. Higher laser power was needed to produce changes in higher temperature liquid crystal at the same wavelength as those for lower temperature samples (32 and 62 mW for the 35−40 and 40−45 °C sample, respectively). Of particular interest is the observation that the photoinduced changes of unit cells in the liquid crystal are not the same but different from cell to cell. A variety of factors may contribute to this inhomogeneity including the difference in sizes of unit cells.

The present study of liquid crystals is just an example illustrating the type of measurements that can be performed using this time-resolved multispectral imaging microscope. The ability

to perform multispectral imaging of sample with a few micrometers size at the milliseconds time scale makes this instrument particularly useful for a variety of measurements that are traditionally difficult to perform. This includes measurements of small-size samples which undergo rapid chemical or biochemical reactions, e.g., activities of a single biological cell. Furthermore, the wavelength region is not limited to the visible as in this study but can be extended to the near- and middle-IR. In fact, by replacing the Dalsa CCD camera with the InGaAs NIR camera, which was previously used in our earlier studies,[3,10,11] NIR multispectral imaging of submicrometer samples in the millisecond time scale can be readily accomplished. These possibilities are currently the subject of our intense investigation.

Acknowledgment is made to the National Institutes of Health, National Center for Research Resources, Biomedical Technology program for financial support of this research.

Received for review July 3, 2000. Accepted November 15, 2000.

AC0007581